Inorganic Chemistry

pubs.acs.org/IC

Article

Systematic Electronic and Structural Studies of 9-Carbene-9-Borafluorene Monoanions and Transformations into Luminescent Boron Spirocycles

Kelsie E. Wentz, Andrew Molino, Lucas A. Freeman, Diane A. Dickie, David J. D. Wilson,* and Robert J. Gilliard, Jr.*

Cite This: https://doi.org/10.1021/acs.inorgchem.2c01945

Read Online

ACCESS | Metrics & More | Article Recommendations | * Supporting Information

ABSTRACT: The impact of the exact spatial arrangement of the alkali metal on the electronic properties of 9-carbene-9-borafluorene monoanions is assessed, and a series of [K][9-CAAC-9-borafluorene] complexes (1−4) have been isolated (CAAC = cyclic(alkyl)(amino) carbene, (2,6-diisopropylphenyl)-4,4-diethyl-2,2-dimethyl-pyrrolidin-5-ylidene). Compound 1, which contains $[B]-K(THF)_3$ interactions, is compared to charge-separated 2−4, which were prepared by capturing the potassium cations with 18-crown-6, 2.2.2-cryptand, or 1,10-phenanthroline. Notably, the ^{11}B NMR spectra of charge-separated borafluorene monoanions 2−4 show distinct low-field signatures compared to 1. Theoretical calculations indicate that charge separation may be exploited to influence the nucleophilic and electron transfer properties of 9-carbene-9-borafluorene monoanions. When [K(2.2.2-cryptand)][9-CAAC-9-borafluorene] (3) is reacted with 9,10-phenanthrenequinone and 1,10-phenanthroline-5,6-dione, the carbene ligand is displaced, and new air-stable R_2BO_2 spirocycles are formed (5 and 6, respectively). Remarkably, compounds 5 and 6 display fluorescence under UV light in both the solid and solution phases with quantum yields of up to 20%. In addition, a drastic red-shift in the emission color is observed in 6 because of the presence of the nitrogen atoms on the phenanthroline moiety. Mechanistic insights into the formation of these spirocycles are also described based on density functional theory calculations.

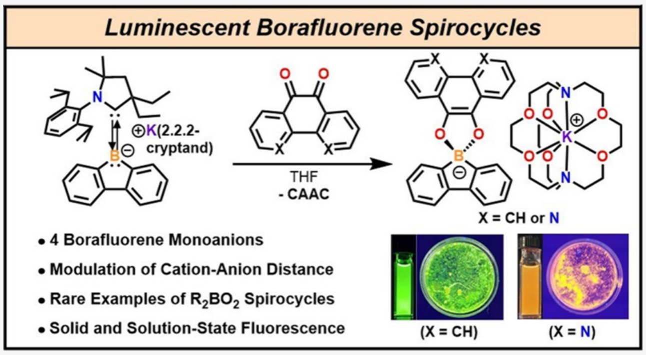

1. INTRODUCTION

Tricoordinate Lewis acidic boron complexes have long been utilized in synthetic chemistry as strong electrophilic reagents for the formation of new olefin polymers,[1−4] substituted aromatics,[5−7] and the functionalization of C−H bonds,[8] which have all been essential in materials-relevant chemical synthesis. However, through chemical reduction reactions, boron-based compounds can be designed such that they become electron-rich nucleophiles. The initial reports on boron nucleophiles (or boryl anions)[9−18] spawned new investigations into understanding the chemistry and reactivity of group 13 Lewis bases (Figure 1a). These compounds are isoelectronic to N-heterocyclic carbenes (NHC) but are weaker sigma-donors[19] and are generally used for the formation of novel B−E bonds (E = transition metal, main-group element, or lanthanide). By stabilizing the E element in low oxidation states, reactivity occurring at the E atom or within the B−E bond can be explored.[20−27] Since the first isolation of the unsaturated boryllithium,[10] structurally unique boryl anions have been reported which have benzannulated backbones and potassium cation interactions with the electron-rich boron atom.[9,12,28−31] Despite this class of compounds being identified nearly 15 years ago, much less is known concerning the chemical reactivity of these species with small molecules compared to the chemistry of the related aluminyl anions,[32−35] which is rapidly emerging. Because of the nature of the bonding within the ion pair (e.g., binding of weakly coordinating atoms, cation-π or other non-covalent interactions, fully charge-separated ions), diverse reactivity can occur. Accordingly, there is still a need for the realization and isolation of electronically and sterically different anionic boryl species as a means to probe reactivity and donor strength at the boron center and their use as a platform for the development of novel boron-containing materials.

Recently, we have been investigating the structure and bonding, reactivity, and materials properties of 9-carbene-9-

Received: June 5, 2022

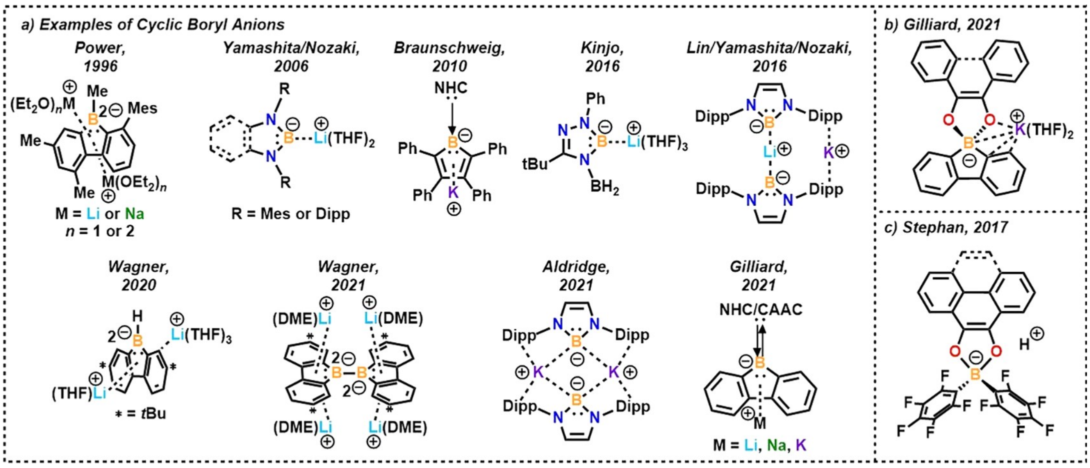

Figure 1. (a) Examples of structurally unique cyclic boryl anions; (b) borafluorene-based spirocycles obtained from 9-carbene-9-borafluorene monoanion and diketones; (c) R_2BO_2 salts prepared via nucleophilic addition to frustrated Lewis pair-stabilized boracyclic radicals.

Scheme 1. Synthesis of [K][9-Carbene-9-borafluorene] Complexes (1−4)

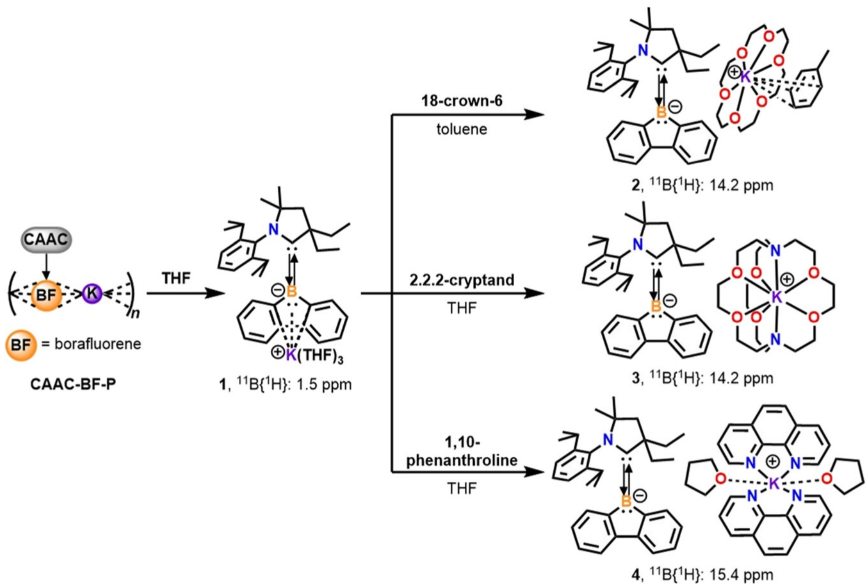

borafluorenes.[14,36−41] While 9-borafluorene has become a popular building block in molecular chemistry,[42] studies of chemically reduced borafluorenes are still rare.[13,14,17,37] Previously, we reported the formation of borafluorene-based spirocycles resulting from the reaction of diketones and 9-carbene-9-borafluorene monoanion (Figure 1b).[14] Although the electronic structures differ significantly, the R_2BO_2 moiety of our closed-shell compounds bear resemblance, in terms of connectivity, to open-shell boracyclic radicals and salts synthesized by Stephan (Figure 1c).[43,44] Most notably, the incorporation of borafluorene in the spirocycle produces fluorescent materials.[14] In light of the novelty of the R_2BO_2 spirocyclic fragment and luminescent properties that can be accessed, we sought to investigate reactions of borafluorene monoanions with other diketones in order to study their optical properties in more detail. This resulted in a need to understand how the spatial arrangement of the alkali metal in 9-carbene-9-borafluorene monoanions affect chemical reactions and the crystallization of various products. Herein, we report a study on the structural and electronic properties of [K][9-CAAC-9-borafluorene] complexes (1−4) (CAAC = (2,6-diisopropylphenyl)-4,4-diethyl-2,2-dimethyl-pyrrolidin-5-ylidene). Charge-separated [K(2.2.2-cryptand)][9-CAAC-9-borafluorene] is used as a building block for the synthesis of boron−oxygen-containing heterocycles 5−6.

2. RESULTS AND DISCUSSION

During our initial studies on the isolation and reactivity of 9-carbene-9-borafluorene monoanions, we often observed solvent- or cation-dependent stability differences and variations in the selectivity for specific products, even in cases where the carbene ligand and alkali metal cation were the same.[14,39] To systematically investigate the possibility of different bonding modes of [K][9-CAAC-9-borafluorene monoanion] (CAAC = (2,6-diisopropylphenyl)-4,4-diethyl-2,2-dimethyl-pyrrolidin-5-ylidene;[45−47] BF = borafluorene) and the role that coordination environment plays in chemical reactions, we first sought to understand the solution-phase behavior of our previously reported [K][9-CAAC-9-BF] coordination polymer (CAAC-BF-P).[14] When CAAC-BF-P is dissolved in tetrahydrofuran (THF) (Scheme 1), the $^{11}B\{^1H\}$ NMR spectrum shows a singlet at 1.5 ppm. Single crystal X-ray diffraction

https://doi.org/10.1021/acs.inorgchem.2c01945
Inorg. Chem. XXXX, XXX, XXX−XXX

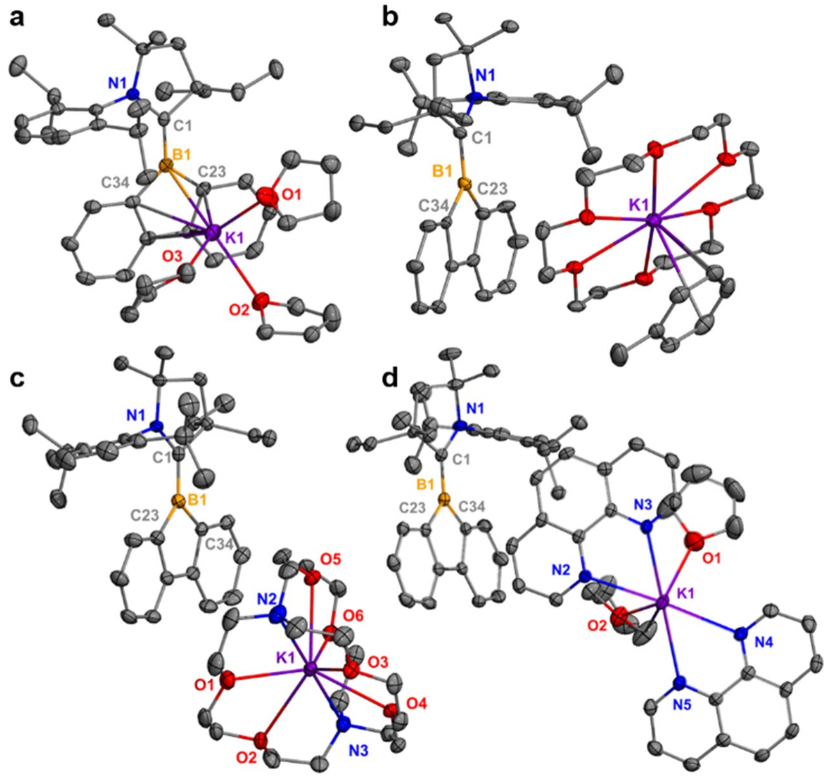

Figure 2. Molecular structures of 1 (a), 2 (b), 3 (c), and 4 (d). Hydrogen atoms omitted for clarity and thermal ellipsoids shown at 50% probability. Selected bond lengths [Å]: 1: B1−C1 1.505(3), B1−C23 1.609(2), B1−C34 1.598(3), B1−K1 3.2363(19); 2: B1−C1 1.519(7), B1−C23 1.586(8), B1−C34 1.617(8), B1−K1 5.911(6); 3: B1−C1 1.495(2), B1−C23 1.601(2), B1−C34 1.616(2), B1−K1 6.891(2); 4: B1−C1 1.504(3), B1−C23 1.607(3), B1−C34 1.600(3), B1−K1 8.095(2).

studies of 1 reveal a $[K(THF)_3]$[9-CAAC-9-BF] structure in which the K atom binds to the central BF ring in a η^5-fashion. In contrast, when compound 1 is reacted with 18-crown-6, 2.2.2-cryptand, or 1,10-phenanthroline, charge-separated ion pairs 2−4 are formed as red solids, which display downfield chemical shifts in the $^{11}B\{^1H\}$ NMR spectra (14.2−15.4 ppm, THF-D_8).

Comparison of the single crystal X-ray diffraction data for 1−4 show that the bond metrics for 1 are similar to free boryl anions (2−4) in the solid state (Figure 2). The B1−C1 bond lengths for 1 [1.505(3)], 2 [1.519(7)], 3 [1.495(2)], and 4 [1.504(3)] are also similar to the previously reported CAAC-BF-P [1.502(5)],[14] and all indicate double bond character between the boron and carbon atoms.

The local paramagnetic contribution (σ^p) is widely understood to be responsible for deshielding nonspherically distributed valence electrons in light nuclei such as boron.[48,49] The paramagnetic term is inversely proportional to the magnitude of the highest occupied molecular orbital−lowest unoccupied molecular orbital (HOMO−LUMO) gap and is especially large in nuclei with asymmetric p and d electron distributions.[50] Theoretical studies were carried out in order to gain insight into the altered electronic characteristics of BF with respect to contact ion distance. A series of BF−K distances were used to calculate the boron chemical shift of 1. In agreement with experimental observations, increasing the distance between the potassium ion and the BF moiety resulted in an increasing downfield chemical shift (δ BF−K(3.1 Å) = 1.89 ppm, δ BF−K(6.6 Å) = 3.95 ppm) (Figure S18). Critically, the paramagnetic contribution (σ^p_{iso}) to the isotropic shielding of ^{11}B was found to increase as the HOMO−LUMO gap steadily decreases in magnitude at greater BF−K distances (Figure 3). The smaller HOMO−LUMO gap results from the destabilization of the HOMO, particularly at BF−K distances greater than 4.5 Å. These

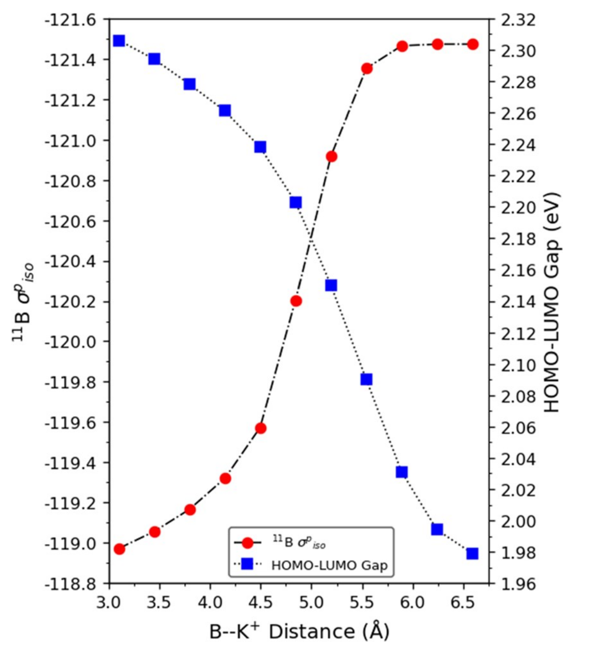

Figure 3. Calculated ^{11}B paramagnetic contribution (σ^p_{iso}) and HOMO−LUMO gaps (eV) with respect to BF−$K(THF)_3$ distance for 1 (TPSSh/pcSseg-2 (CPCM, THF)).

https://doi.org/10.1021/acs.inorgchem.2c01945
Inorg. Chem. XXXX, XXX, XXX−XXX

results indicate that different-sized chelating agents may be utilized to control the HOMO energy of 9-CAAC-9-BF monoanion, altering its nucleophilic and reducing properties (vide infra).

We hypothesized that the use of the charge-separated borafluorene monoanion 3 as a starting material for reactions with 9,10-phenanthrenequinone and 1,10-phenanthroline-5,6-dione would generate borafluorene spirocycles with varied photophysical properties. Upon addition of 9,10-phenanthrenequinone or 1,10-phenanthroline-5,6-dione to 3, an immediate color change from deep red to orange was observed, indicative of the formation of 5 and 6, respectively (Scheme 2).

Scheme 2. Displacement of the CAAC Ligand by 9,10-Phenanthrenequinone and 1,10-Phenanthroline-5,6-dione To Form Spirocyclic Borafluorenes (5−6)

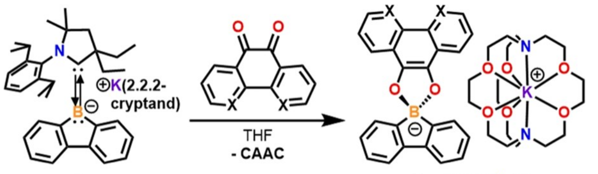

In both cases, the CAAC ligand was displaced, and borafluorene spirocycles 5 and 6 were characterized by distinct downfield chemical shifts in the ^{11}B NMR spectra at 16.2 and 16.6 ppm, respectively. Yellow and orange air-stable single crystals of 5 and 6 were grown from concentrated solutions in THF with a couple of drops of hexanes added. In both molecules, charge-separated boron-based spirocycles with no potassium contacts were observed, which differ from our previously reported borafluorene spirocycles that exist as coordination polymers (Figure 4).[14] Additionally, the B−O bonds of 5 and 6 range from 1.513(14) to 1.533(2) Å, and are close in length to the sum of the covalent single bond radii (R(B−O) = 1.50 Å),[51] indicative of single bond character. The placement of the nitrogen atoms on 6 leaves a site for potential binding to other elements to generate mixed metal systems. Compound 6 is particularly interesting as 1,10-phenanthroline complexes have been used for various technologies including analytical probes.[52−54] Because of the higher quantum yields of 6 ($\Phi_{solution}$ = 4%) compared to the weakly luminescent parent phenanthroline ($\Phi_{solution}$ = 0.8%),[52] complexes similar to 6 should open up new possibilities in molecular materials applications.

The reactivity of nucleophiles with monocyclic benzoquinones is well-documented to undergo addition and substitution reactions at the carbonyl-alpha positions facilitated by the ability to form enolate anions.[55] Because of the absence of acidic hydrogen atoms at the positions alpha to the carbonyl, nucleophilic reactivity is not observed with saturated polycyclic quinones.[56] Recently, we demonstrated that 1 may serve as a single-electron reducing agent with diselenides to undergo subsequent radical coupling.[39] Single-electron transfer (SET) can occur spontaneously, provided the energies of the donor HOMO and acceptor LUMO are close. Quinones are especially susceptible to SET reactions as the carbonyl π^* orbital is easily reduced to generate an electronically stabilized ketyl radical anion.[57] Furthermore, it has been observed that the reactivity of quinones with electron-rich species occurs via electron-transfer routes, resulting in cyclization products similar to those described herein.[58−62]

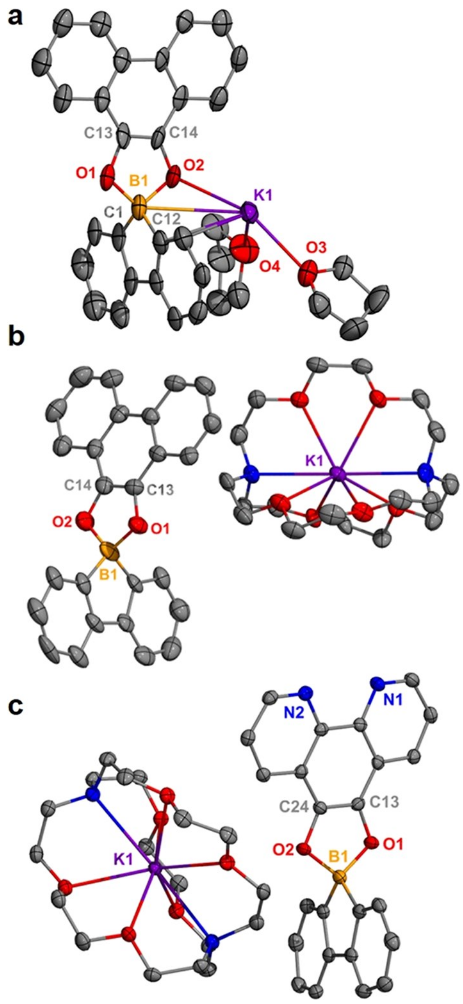

Figure 4. Molecular structures of B-phen (a),[14] 5 (b), and 6 (c). Hydrogen atoms omitted for clarity and thermal ellipsoids shown at 50% probability. Selected bond lengths [Å]: B-phen: B1−O1: 1.52(3); B1−O2: 1.57(3); O1−C13: 1.42(2); O2−C14: 1.35(2); C13−C14: 1.30(3); 5: B1−O1 1.525(13), B1−O2 1.513(14), O1−C13 1.362(11), O2−C14 1.356(12), C13−C14 1.352(14); 6: B1−O1 1.533(2), B1−O2 1.532(2), O1−C13 1.348(2), O2−C24 1.49(2), C13−C24 1.364(2).

Theoretical calculations were utilized to determine a possible mechanism for the formation of spirocycles 5 and 6. We first sought to model the energetic feasibility of an electron transfer pathway. The $\mathrm{HOMO}_{(9\text{-CAAC-9-BF})}$−$\mathrm{LUMO}_{(9,10\text{-phenanthrenequinone})}$ gap was calculated to be 0.59 eV ($\mathrm{HOMO}_{(9\text{-CAAC-9-BF})}$−$\mathrm{LUMO}_{(1,10\text{-phenanthroline-5,6-dione})}$ = 0.73 eV), well within the range for spontaneous electron transfer (Figure 5).[63] Further support for a SET process is revealed when comparing the relative free energies of the reactant encounter complexes. The open-shell singlet reactant complex (^{OSS}RC) was calculated to be lower in energy than the closed-shell singlet analogue, relative to the free reactants ($\Delta\Delta G$ = −53 kJ mol^{-1}) (Figure 6). A transition state was located describing the formation of an adduct (Int1) between boron and one of the oxygen atoms (TS1, $\Delta G^{\ddagger}$ = +67 kJ mol^{-1}). In contrast to free quinone, the C−C bond linking the carbonyl groups in Int1 is shorter by 0.129 Å, while the unbound carbonyl bond is longer by +0.060 Å. The HOMO of Int1 is localized to the quinone moiety, displaying significant π-bonding character across both carbonyl α-carbons (Figure

https://doi.org/10.1021/acs.inorgchem.2c01945
Inorg. Chem. XXXX, XXX, XXX−XXX

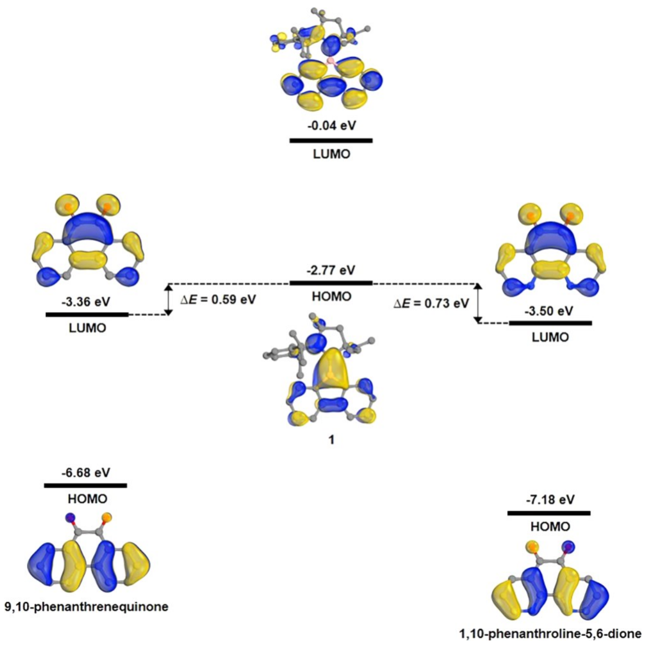

Figure 5. Calculated frontier molecular orbital energies of $[9\text{-CAAC-9-BF}]^-$ and quinone substrates 9,10-phenanthrenequinone and 1,10-phenanthroline-5,6-dione (B3LYP-D3(BJ)/def2-TZVP//B3LYP-D3(BJ)/def2-SVP (CPCM, THF)).

S19). The geometry and electronic structure of Int1 are characteristic of an enolate intermediate. Furthermore, the unique resonance stabilizing effects of enolate anions may explain the high stability of anion Int1 relative to the reactants. Following the formation of Int1, stepwise elimination of CAAC (TS2, $\Delta G^{\ddagger}$ = +98 kJ mol^{-1}) and subsequent intramolecular cyclization (TS3, $\Delta G^{\ddagger}$ = +67 kJ mol^{-1}) result in the spirocyclic product (ΔG_{rxn} = −193 kJ mol^{-1}).

UV−vis and fluorescence studies were performed to investigate the photophysical characteristics of the borafluorene spirocycles in the solution phase. Absorption maxima for 5 and 6 are observed at 390 and 414 nm, respectively, with red-shifted emission wavelengths for 5 and 6 at 517 and 569 nm (Figure 7). These absorption and emission values are consistent with the previously reported potassium-coordinated borafluorene spirocycles (B-benzil and B-phen − see Table 1 for structures).[14] However, under UV light, 5 displays a bright green color while 6 is orange.

To quantify luminescence, quantum yield (QY) measurements were obtained in the solution and solid states of the borafluorene spirocycles. Expectedly, B-phen has the highest QY in solution phase because of the more rigid structure compared to B-benzil (Table 1). However, compound 5 has a higher QY in the solid state, likely due to aggregation-induced emission. Time-dependent density functional theory (TD-DFT − ωB97X/def2-TZVP, CPCM(THF)) analysis indicates that the lowest energy transition for 5 and 6 is associated with $\pi \rightarrow \pi^*$ excitations centered on the quinone moieties (Figures S20−22). Spirocycles 5 and 6 possess C_{2v} symmetry, resulting in weak symmetry forbidden charge-transfer transitions between the quinone and borafluorene moieties (Table S3). While the QYs for 6 are low, those of 5 are higher, and both

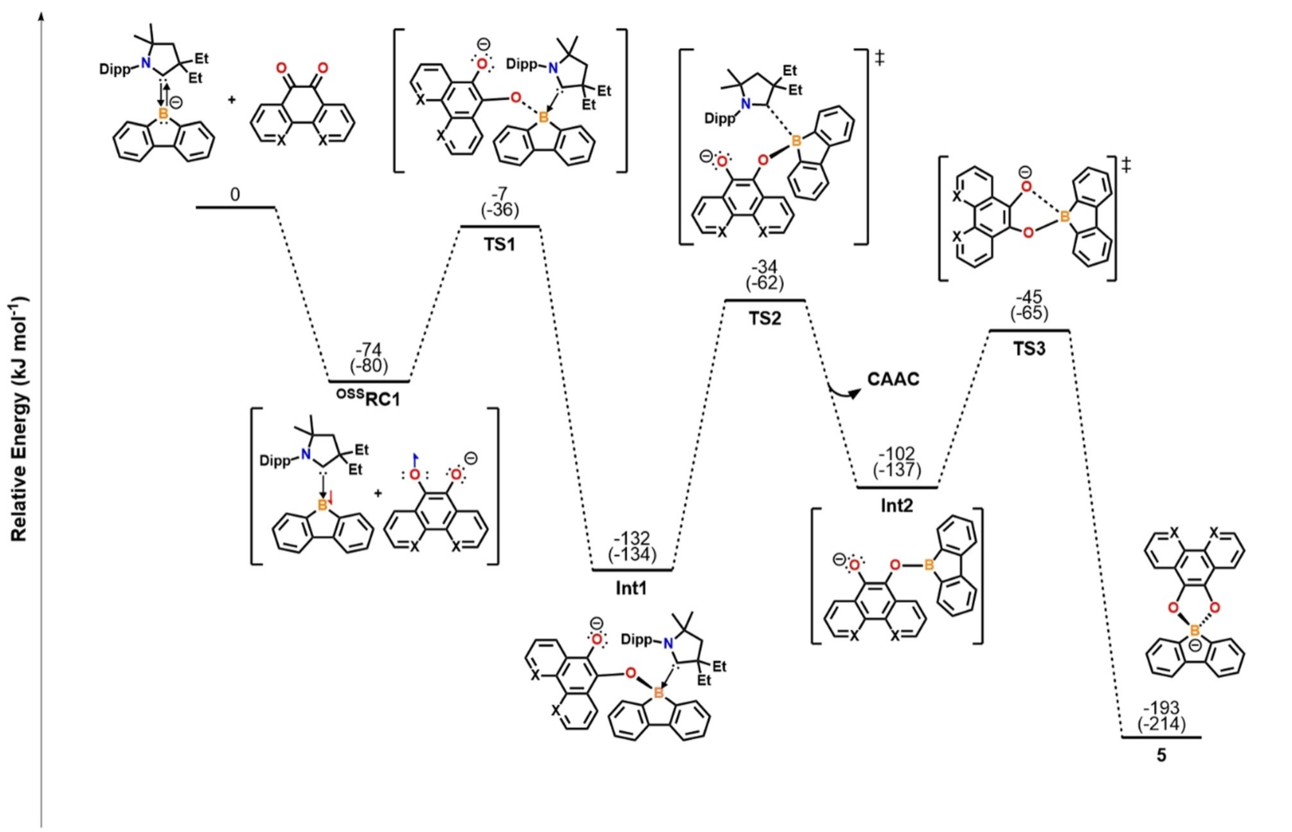

Figure 6. Calculated free energies relative to reactants (ΔG, kJ mol^{-1}) for the reactivity of $[9\text{-CAAC-9-BF}]^-$ and 9,10-phenanthrenequinone (B3LYP-D3(BJ)/def2-TZVP//B3LYP-D3(BJ)/def2-SVP (SMD, THF)). Values in parentheses correspond to the reactivity of $[9\text{-CAAC-9-BF}]^-$ with 1,10-phenanthroline-5,6-dione.

https://doi.org/10.1021/acs.inorgchem.2c01945
Inorg. Chem. XXXX, XXX, XXX−XXX

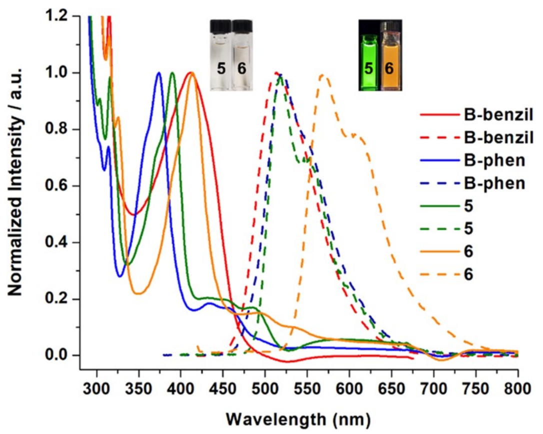

Figure 7. Normalized absorption (solid line) and emission (dashed line) spectra of B-benzil (red) B-phen (blue), 5 (green), and 6 (orange). Samples were dissolved in THF and ran at room temperature. Excitation wavelengths: B-benzil and 6 (λ_{ex} = 410 nm); B-phen (λ_{ex} = 370 nm) and 5 (λ_{ex} = 390 nm).

Table 1. Comparison of QYs in THF Solutions and the Solid State

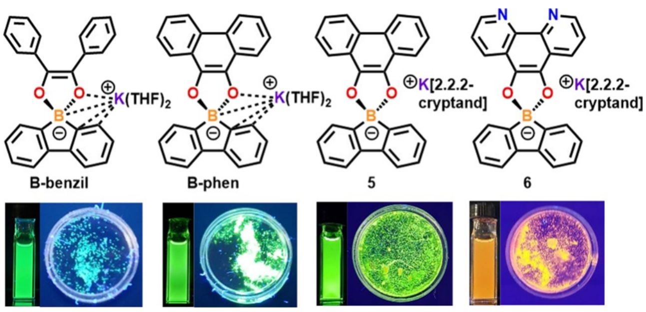

compound	$\Phi_F^{(solution)}$/%[a]	$\Phi_F^{(solid)}$/%[a]
B-benzil	21	1
B-phen	37	6
5	20	16
6	4	4

[a]Absolute QYs determined using an integrating sphere. Digital images of solution and solid-state luminescence are shown under 365 nm UV light.

the borafluorene and quinone moieties possess highly conjugated structures that may be easily functionalized. Therefore, we envisage the utility of these spirocycles as new frameworks for which charge-transfer complexes may be built upon.

3. CONCLUSIONS

In summary, we report structurally unique [K][9-CAAC-9-BF] complexes (1−4). Charge-separated compounds 2−4 with potassium counterions chelated by 18-crown-6, 2.2.2-cryptand, and 1,10-phenanthroline are identified by distinct low-field ^{11}B NMR chemical shifts compared to compound 1 where the K atom is coordinated to the central boron ring. Theoretical modeling identifies that these low-field signals are due to a large paramagnetic contribution at boron as a result of reduced HOMO−LUMO gaps in charge-separated borafluorenes. The ability to easily tune the HOMO of 9-carbene-9-borafluorene monoanions not only allows for the modification of the anion's electronic structure but may also prove useful as a means to control reactivity.[14,39] Moreover, when reacting 3 with 9,10-phenanthrenequione and 1,10-phenanthroline-5,6-dione, novel charge-separated boron spirocycles (5 and 6) are synthesized via carbene elimination, with computational mechanistic studies suggesting this reactivity proceeds via an electron-transfer mechanism. Compounds 5 and 6 display bright green and orange luminescence under UV light and are air-stable in the solid state. The presence of nitrogen atoms on the phenanthroline moiety of 6 leads to a red-shifted emission. Because of the open biding site, compounds similar to 6 may be useful in the preparation of other coordination complexes. Additional reactivity studies with the charge-separated borafluorene monoanions and spirocycles are currently underway in our laboratory and will be reported in due course.

4. EXPERIMENTAL SECTION

4.1. General Procedures. All experiments were carried out under an inert atmosphere of argon using an MBRAUN LABmaster glovebox equipped with a −37 °C freezer. The solvents were purified by distillation over sodium and benzophenone. THF-d_8 for NMR experiments was purified by distillation over sodium and stored over Na/K under an inert atmosphere. Glassware was oven-dried at 190 °C overnight. The NMR spectra were recorded at room temperature on a Varian 600 MHz spectrometer. Proton and carbon chemical shifts are reported in ppm and referenced using the residual proton and carbon signals of the deuterated solvent (^{1}H: THF-d_8 − δ = 3.58; ^{13}C: THF-d_8 − δ = 67.6), while boron chemical shifts are referenced to an external standard (^{11}B: BF_3•Et_2O − δ = 0.0). Because of the borosilicate NMR probe, a large broad peak is observed at approximately 25 to −25 ppm in the ^{11}B NMR spectra. The UV−visible and fluorescence spectra were recorded on a Cary 60 UV−vis spectrophotometer and a Cary Eclipse fluorescence spectrophotometer. Sample solutions were prepared in THF in 1 cm square air-free quartz cuvettes. Absolute fluorescence QYs were obtained using a Hamamatsu C11347-11 Quantaurus-QY Absolute PL QY spectrometer. Samples were prepared in a glovebox using quartz Petri dishes (single crystals) or 1 cm square quartz cuvettes (solutions). The solutions were prepared in THF, and the data were collected with absorbance values less than 0.1. Elemental analyses were performed on a Perkin-Elmer 2400 Series II analyzer. 1,10-Phenanthroline, 9,10-phenanthrenequinone, 1,10-phenanthroline-5,6-dione, and 2.2.2 cryptand were purchased from Sigma Aldrich and used as received. 18-Crown-6 was purchased from Sigma Aldrich and was recrystallized from minimal toluene at −37 °C and dried under reduced pressure before use. Compound 1[14] was prepared according to the previous literature from 2,6-diisopropylphenyl)-4,4-diethyl-2,2-dimethyl-pyrrolidin-5-ylidene and 9-bromo-9-borafluorene. Single crystals of 1 for X-ray diffraction studies were grown from a concentrated THF solution with a few added drops of hexanes and storage at −37 °C.

4.2. Synthesis of Compound 2. In a vial, 1 (25.0 mg, 0.0483 mmol) and 18-crown-6 (12.8 mg, 0.0483 mmol) were dissolved in toluene (5 mL). The solution was then filtered through a 0.45 μm polytetrafluoroethylene (PTFE) syringe filter to remove any residual solids. Dark red rod-shaped crystals were obtained and further dried under vacuum (13.3 mg, 35% yield). ^{1}H NMR (600 MHz, THF-d_8, 298 K) δ = 7.90 (d, J = 7.4 Hz, 1H, ArH), 7.49 (d, J = 8.4 Hz, 1H, ArH), 7.36 (d, J = 7.5 Hz, 1H, ArH), 7.22 (t, J = 7.7 Hz, 1H, ArH), 7.10 (d, J = 7.7 Hz, 2H, ArH), 6.69 (t, J = 7.4 Hz, 1H, ArH), 6.50 (t, J = 7.0 Hz, 2H, ArH), 6.29 (t, J = 7.0 Hz, 1H, ArH), 6.00 (t, J = 8.0 Hz, 1H, ArH), 4.75 (d, J = 8.4 Hz, 1H, ArH), 3.68 (hept, J = 7.0 Hz, 2H, $CH(CH_3)_2$), 3.24 (s, 24H, 18-c-6), 2.52 (m, 2H, CH_2CH_3), 2.38 (m, 2H, CH_2CH_3), 2.01 (s, 2H, CH_2) 1.17 (m, 12H, $CH(CH_3)_2$/$(CH_3)_2$), 1.08 (t, J = 7.3 Hz, 6H, CH_2CH_3), 0.81 ppm (d, J = 6.6 Hz, 6H, $CH(CH_3)_2$); ^{13}C{^{1}H} NMR (151 MHz, THF-d_8, 298 K) δ = 153.9, 144.2, 133.2, 126.8, 124.7, 121.7, 121.0, 117.6, 117.0, 116.6, 116.3, 71.1, 53.06, 51.00, 32.0, 31.7, 29.7, 27.2, 11.0 ppm; ^{11}B{^{1}H} NMR (193 MHz, THF-d_8, 298 K) δ = 14.2 ppm. Anal calcd for

https://doi.org/10.1021/acs.inorgchem.2c01945
Inorg. Chem. XXXX, XXX, XXX−XXX

$C_{53}H_{75}BKNO_6$: C, 72.99; H, 8.67; N, 1.61%. Found: C, 72.88; H, 8.66; N, 1.70%.

4.3. Synthesis of Compound 3. In a vial, 1 (25.0 mg, 0.0483 mmol) and 2.2.2 cryptand (18.2 mg, 0.0483 mmol) were dissolved in toluene (5 mL). The solution was then filtered through a 0.45 μm PTFE syringe filter to remove any residual solids. The deep red solution was concentrated to ∼2 mL under reduced pressure and stored at room temperature for recrystallization. Dark red block-shaped crystals were obtained and further dried under vacuum (34.3 mg, 79% yield). ^{1}H NMR (600 MHz, THF-d_8, 298 K) δ = 7.90 (d, J = 7.9 Hz, 1H, ArH), 7.51 (d, J = 8.3 Hz, 1H, ArH), 7.37 (d, J = 8.5 Hz, 1H, ArH), 6.68 (t, J = 7.9 Hz, 1H, ArH), 6.51 (t, J = 7.0 Hz, 1H, ArH), 6.30 (t, J = 7.0 Hz, 1H, ArH), 6.00 (t, J = 8.0 Hz, 1H, ArH), 4.75 (d, J = 7.9 Hz, 1H, ArH), 3.69 (hept, J = 6.7 Hz, 2H, CH(CH$_3$)$_2$), 3.23 (m, 24H, crypt), 2.53 (m, 2H, CH_2CH$_3$), 2.39 (m, 2H, CH_2CH$_3$), 2.23 (br s, 12H, crypt), 2.02 (s, 2H, CH_2), 1.18 (m, 12H, CH(CH_3)$_2$/(CH_3)$_2$), 1.09 (t, J = 7.3 Hz, 6H, CH$_2$CH_3), 0.83 ppm (d, J = 6.6 Hz, 6H, CH(CH_3)$_2$); ^{13}C{^{1}H} NMR (151 MHz, THF-d_8, 298 K) δ = 154.0, 138.6, 134.1, 133.2, 129.8, 129.1, 126.8, 126.2, 124.7, 121.7, 121.2, 121.1, 117.7, 117.0, 116.6, 116.4, 71.3, 68.5, 65.6, 54.7, 53.0, 51.0, 32.0, 31.7, 29.7, 27.3, 11.0 ppm; ^{11}B{^{1}H} NMR (193 MHz, THF-d_8, 298 K) δ = 14.2 ppm. Anal calcd for $C_{52}H_{79}BKN_3O_6$: C, 70.01; H, 8.93; N, 4.71%. Found: C, 70.06; H, 9.20; N, 4.61%.

4.4. Synthesis of Compound 4. In a vial, 1 (50.0 mg, 0.0966 mol) was dissolved in THF (4 mL), and 1,10-phenanthroline (34.8 mg, 0.193 mmol) was then added. The reaction was stirred at room temperature for 4 h. A few drops of hexanes were added to the solution, and after storage at −37 °C, red needle-shaped single crystals were obtained (55.0 mg, 56%). ^{1}H NMR (600 MHz, THF-d_8) δ 8.72 (d, J = 2.7 Hz, 4H, ArH), 8.24 (br s, 4H, ArH) 8.03 (d, J = 7.5 Hz, 1H), 7.78 (s, 4H, ArH) 7.49 (m, 6H, ArH), 7.28 (t, J = 7.7 Hz, 1H, ArH), 7.13 (d, J = 8.0 Hz, 2H, ArH), 6.79 (t, J = 8.0 Hz, 1H, ArH), 6.55 (t, J = 7.2 Hz, 1H, ArH), 6.41 (t, J = 7.7 Hz, 1H, ArH), 6.16 (t, J = 7.9 Hz, 1H, ArH), 4.84 (d, J = 7.8 Hz, 1H, ArH), 3.62 (m, 8H, OCH_2CH$_2$), 2.51 (m, 2H, CH_2CH$_3$), 2.37 (m, 2H, CH_2CH$_3$), 2.01 (s, 2H, CH_2), 1.77 (m, 8H, OCH$_2$CH_2), 1.16 (m, 12H, CH(CH_3)$_2$/(CH_3)$_2$), 1.01 (t, J = 7.3 Hz, 6H, CH$_2$CH_3), 0.76 (d, J = 6.6 Hz, 6H, CH(CH_3)$_2$); ^{13}C{^{1}H} NMR (151 MHz, THF-d_8, 298 K) δ = 185.8, 153.6, 150.7, 147.3, 137.1, 134.5, 133.3, 127.6, 127.3, 125.0, 122.4, 121.8, 118.3, 117.6, 117.3, 117.0, 111.2, 99.9, 50.5, 32.0, 31.6, 29.7, 27.0, 24.8, 10.8; ^{11}B{^{1}H} NMR (193 MHz, THF-d_8, 298 K) δ = 15.4 ppm. Anal calcd for $C_{66}H_{75}BKN_5O_2$: C, 77.70; H, 7.41; N, 6.86%. Found: C, 77.48; H, 7.70; N, 6.72%.

4.5. Synthesis of Compound 5. In a vial, 1 (50.0 mg, 0.0966 mmol) and 2.2.2 cryptand (36.4 mg, 0.0966 mmol) were dissolved in THF (5 mL), and 9,10-phenanthrenequinone (20.1 mg, 0.0966 mmol) was then added. The deep red solution immediately turned orange in color and was stirred at room temperature for 2 h. During that time, yellow fluorescent crystals precipitated out of solution. The yellow crystals were collected via filtration, washed with hexanes (5 mL), and dried under reduced pressure (53.2 mg, 70% yield). Single crystals were grown from a concentrated THF solution and with a few drops of hexanes added. ^{1}H NMR (600 MHz, THF-d_8, 298 K) δ = 8.57 (d, J = 8.2 Hz, 2H, ArH), 7.99 (dd, J = 8.1, 1.4 Hz, 2H, ArH), 7.42 (d, J = 7.6 Hz, 2H, ArH), 7.30 (m, 4H, ArH), 7.16 (ddd, J = 8.2, 6.7, 1.3 Hz, 2H, ArH), 6.96 (td, J = 7.4, 1.3 Hz, 2H, ArH), 6.83 (td, J = 7.1, 0.9 Hz, 2H, ArH), 3.45 (s, 12H, crypt), 3.38 (m, 12H, crypt), 2.38 (m, 12H, crypt). ^{13}C{^{1}H} NMR (151 MHz, THF-d_8, 298 K) δ = 131.5, 126.5, 126.4, 126.3, 125.4, 125.0, 123.4, 121.8, 120.6, 118.4, 118.2, 109.1, 71.4, 68.6, 54.9 ppm. Due to peak broadening attributed to quadrupolar relaxation, we were unable to observe the two sp^2 carbon atoms bound to boron for this compound.; ^{11}B{^{1}H} NMR (193 MHz, THF-d_8, 298 K) δ = 16.2 ppm. Anal calcd for $C_{44}H_{52}BKN_2O_8$: C, 67.17; H, 6.66; N, 3.56%. Found: C, 66.95; H, 6.95; N, 3.26%.

4.6. Synthesis of Compound 6. In a vial, 1 (50.0 mg, 0.0966 mmol) and 2.2.2 cryptand (36.4 mg, 0.0966 mmol) were dissolved in THF (4 mL). 1,10-Phenanthroline-5,6-dione (20.3 mg, 0.0966 mmol) was then added. The deep red solution quickly turned orange in color and was stirred at room temperature for 4 h. The insoluble solids were removed via filtration through a 0.45 μm PTFE syringe filter. A few drops of hexanes were added to the filtrate and orange single crystals were grown at room temperature after slow evaporation (38.4 mg, 50%). ^{1}H NMR (600 MHz, THF-d_8, 298 K) δ = 8.68 (dd, J = 4.1, 1.8 Hz, 2H, ArH), 8.28 (dd, J = 8.1, 1.8 Hz, 2H, ArH), 7.43 (d, J = 7.5 Hz, 2H, ArH), 7.30 (m, 2H, ArH), 6.99 (td, J = 7.4, 1.3 Hz, 2H, ArH), 6.84 (td, J = 7.1, 1.0 Hz, 2H, ArH), 3.45 (s, 12H, crypt), 3.39 (m, 12H, crypt), 2.39 ppm (m, 12H, crypt). ^{13}C NMR (151 MHz, THF-d_8, 298 K) δ = 149.9, 145.9, 144.2, 141.9, 131.3, 128.3, 126.8, 126.5, 121.3, 118.5, 71.4, 68.6, 54.9 ppm. Because of peak broadening attributed to quadrupolar relaxation, we were unable to observe the two sp^2 carbon atoms bound to boron for this compound; ^{11}B{^{1}H} NMR (193 MHz, THF-d_8, 298 K) δ = 16.6 ppm. Anal calcd for $C_{42}H_{50}BKN_4O_8$•1/2(hexanes): C, 64.89; H, 7.02; N, 6.73%. Found: C, 65.00; H, 6.74; N, 6.48%.

4.7. Theoretical Calculations. Geometry optimizations were performed at the B3LYP-D3(BJ)/def2-SVP (CPCM, THF) level of theory in Orca 5.0.2.[64] All optimizations utilized the resolution of identity approximation for both Coulomb and Hartree-Fock exchange integrals and a 590-point integration grid. Harmonic frequency calculations were conducted analytically to confirm that optimized geometries were minima on the potential energy surface. Isotropic chemical shielding values for ^{11}B were calculated relative to $BF_3O(Et)_2$. All NMR calculations were performed using Orca 5.0.2 at the TPSSh/pcSseg-2//B3LYP-D3(BJ)/def2-SVP (CPCM, THF) level of theory with GIAO. We note that the calculations of nuclear shielding values are extremely sensitive to the molecular geometry and that, in experimental conditions, the systems are highly dynamic. Nevertheless, the theoretical results for the nuclear shielding values of the constrained scans reported here agree with the observed experimental trends. CM5 partial atomic charges and Wiberg bond indices were calculated from the optimized geometries using Gaussian 16 rev C.01 and NBO 6.0 at the B3LYP-D3(BJ)/def2-TZVP level of theory inclusive of PCM solvation (SMD model) with parameters for THF solvation.[65−67] TD-DFT calculations were performed using ORCA 5.0.2 at the ωB97X/def2-TZVP (CPCM, THF) level of theory.

ASSOCIATED CONTENT

* Supporting Information

The Supporting Information is available free of charge at https://pubs.acs.org/doi/10.1021/acs.inorgchem.2c01945.

NMR spectra for compounds 2−6; X-ray refinement details; and computational details (PDF)

Accession Codes

CCDC 2157309−2157314 contain the supplementary crystallographic data for this paper. These data can be obtained free of charge via www.ccdc.cam.ac.uk/data_request/cif, or by emailing data_request@ccdc.cam.ac.uk, or by contacting The Cambridge Crystallographic Data Centre, 12 Union Road, Cambridge CB2 1EZ, UK; fax: +44 1223 336033.

AUTHOR INFORMATION

Corresponding Authors

David J. D. Wilson − *Department of Biochemistry and Chemistry, La Trobe Institute for Molecular Science, La Trobe University, Melbourne 3086 Victoria, Australia;* orcid.org/0000-0002-0007-4486; Email: david.wilson@latrobe.edu.au

Robert J. Gilliard, Jr. − *Department of Chemistry, University of Virginia, Charlottesville 22904 Virginia, United States;* orcid.org/0000-0002-8830-1064; Email: rjg8s@virginia.edu

https://doi.org/10.1021/acs.inorgchem.2c01945
Inorg. Chem. XXXX, XXX, XXX−XXX

Authors

Kelsie E. Wentz − *Department of Chemistry, University of Virginia, Charlottesville 22904 Virginia, United States;* orcid.org/0000-0002-0464-8010

Andrew Molino − *Department of Biochemistry and Chemistry, La Trobe Institute for Molecular Science, La Trobe University, Melbourne 3086 Victoria, Australia;* orcid.org/0000-0002-0954-9054

Lucas A. Freeman − *Department of Chemistry, University of Virginia, Charlottesville 22904 Virginia, United States;* orcid.org/0000-0003-0962-8921

Diane A. Dickie − *Department of Chemistry, University of Virginia, Charlottesville 22904 Virginia, United States;* orcid.org/0000-0003-0939-3309

Complete contact information is available at: https://pubs.acs.org/10.1021/acs.inorgchem.2c01945

Notes

The authors declare no competing financial interest.

ACKNOWLEDGMENTS

The authors acknowledge the University of Virginia and the National Science Foundation Chemical Synthesis (CHE 2046544) and Major Research Instrumentation (CHE 2018870) programs for support of this work. R.J.G. acknowledges additional laboratory support through a Beckman Young Investigator Award from the Arnold and Mabel Beckman Foundation. Generous allocation of computing resources from the National Computational Infrastructure (NCI), Intersect, and La Trobe University is also acknowledged.

REFERENCES

(1) Chen, E. Y.-X.; Marks, T. J. Cocatalysts for Metal-Catalyzed Olefin Polymerization: Activators, Activation Processes, and Structure−Activity Relationships. *Chem. Rev.* 2000, *100*, 1391−1434.

(2) Chen, Y.-X.; Stern, C. L.; Yang, S.; Marks, T. J. Organo-Lewis Acids As Cocatalysts in Cationic Metallocene Polymerization Catalysis. Unusual Characteristics of Sterically Encumbered Tris(perfluorobiphenyl)borane. *J. Am. Chem. Soc.* 1996, *118*, 12451−12452.

(3) Yang, X.; Stern, C. L.; Marks, T. J. Cation-like homogeneous olefin polymerization catalysts based upon zirconocene alkyls and tris(pentafluorophenyl)borane. *J. Am. Chem. Soc.* 1991, *113*, 3623−3625.

(4) Yang, X.; Stern, C. L.; Marks, T. J. Cationic Zirconocene Olefin Polymerization Catalysts Based on the Organo-Lewis Acid Tris(pentafluorophenyl)borane. A Synthetic,Structural, Solution Dynamic, and Polymerization Catalytic Study. *J. Am. Chem. Soc.* 1994, *116*, 10015−10031.

(5) Ishihara, K.; Hananki, N.; Yamamoto, H. Tris(pentafluorophenyl) boron as a New Efficient, Air Stable, and Water Tolerant Catalyst in the Aldol-Type and Michael Reactions. *Synlett* 1993, *1993*, 577−579.

(6) Parks, D. J.; Piers, W. E. Tris(pentafluorophenyl)boron-Catalyzed Hydrosilation of Aromatic Aldehydes, Ketones, and Esters. *J. Am. Chem. Soc.* 1996, *118*, 9440−9441.

(7) Sowa, F. J.; Hennion, G. F.; Nieuwland, J. A. Organic Reactions with Boron Fluoride. IX. The Alkylation of Phenol with Alcohols1. *J. Am. Chem. Soc.* 1935, *57*, 709−711.

(8) Ma, Y.; Lou, S.-J.; Hou, Z. Electron-deficient boron-based catalysts for C−H bond functionalisation. *Chem. Soc. Rev.* 2021, *50*, 1945−1967.

(9) Segawa, Y.; Suzuki, Y.; Yamashita, M.; Nozaki, K. Chemistry of Boryllithium: Synthesis, Structure, and Reactivity. *J. Am. Chem. Soc.* 2008, *130*, 16069−16079.

(10) Segawa, Y.; Yamashita, M.; Nozaki, K. Boryllithium: Isolation, Characterization, and Reactivity as a Boryl Anion. *Science* 2006, *314*, 113−115.

(11) Yamashita, M.; Nozaki, K., Boryl Anions. In *Synthesis and Application of Organoboron Compounds*, Fernández, E.; Whiting, A., Eds.; Springer International Publishing: Cham, 2015; pp 1−37.

(12) Braunschweig, H.; Chiu, C.-W.; Radacki, K.; Kupfer, T. Synthesis and Structure of a Carbene-Stabilized π-Boryl Anion. *Angew. Chem., Int. Ed.* 2010, *49*, 2041−2044.

(13) Gilmer, J.; Budy, H.; Kaese, T.; Bolte, M.; Lerner, H.-W.; Wagner, M. The 9H-9-Borafluorene Dianion: A Surrogate for Elusive Diarylboryl Anion Nucleophiles. *Angew. Chem., Int. Ed.* 2020, *59*, 5621−5625.

(14) Wentz, K. E.; Molino, A.; Weisflog, S. L.; Kaur, A.; Dickie, D. A.; Wilson, D. J. D.; Gilliard, R. J., Jr. Stabilization of the Elusive 9-Carbene-9-Borafluorene Monoanion. *Angew. Chem., Int. Ed.* 2021, *60*, 13065−13072.

(15) Budy, H.; Gilmer, J.; Trageser, T.; Wagner, M. Anionic Organoboranes: Delicate Flowers Worth Caring for. *Eur. J. Inorg. Chem.* 2020, *2020*, 4148−4162.

(16) Kinjo, R.; Donnadieu, B.; Celik, M. A.; Frenking, G.; Bertrand, G. Synthesis and Characterization of a Neutral Tricoordinate Organoboron Isoelectronic with Amines. *Science* 2011, *333*, 610−613.

(17) Budy, H.; Kaese, T.; Bolte, M.; Lerner, H.-W.; Wagner, M. A Chemiluminescent Tetraaryl Diborane(4) Tetraanion. *Angew. Chem., Int. Ed.* 2021, *60*, 19397−19405.

(18) Grigsby, W. J.; Power, P. P. Isolation and Reduction of Sterically Encumbered Arylboron Dihalides: Novel Boranediyl Insertion into C−C σ-Bonds. *J. Am. Chem. Soc.* 1996, *118*, 7981−7988.

(19) Romeo, L. J.; Kaur, A.; Wilson, D. J. D.; Martin, C. D.; Dutton, J. L. Evaluation of the σ-Donating and π-Accepting Properties of N-Heterocyclic Boryl Anions. *Inorg. Chem.* 2019, *58*, 16500−16509.

(20) Li, S.; Cheng, J.; Chen, Y.; Nishiura, M.; Hou, Z. Rare Earth Metal Boryl Complexes: Synthesis, Structure, and Insertion of a Carbodiimide and Carbon Monoxide. *Angew. Chem., Int. Ed.* 2011, *50*, 6360−6363.

(21) Protchenko, A. V.; Dange, D.; Blake, M. P.; Schwarz, A. D.; Jones, C.; Mountford, P.; Aldridge, S. Oxidative Bond Formation and Reductive Bond Cleavage at Main Group Metal Centers: Reactivity of Five-Valence-Electron MX2 Radicals. *J. Am. Chem. Soc.* 2014, *136*, 10902−10905.

(22) Bertermann, R.; Braunschweig, H.; Dewhurst, R. D.; Hörl, C.; Kramer, T.; Krummenacher, I. Evidence for Extensive Single-Electron-Transfer Chemistry in Boryl Anions: Isolation and Reactivity of a Neutral Borole Radical. *Angew. Chem., Int. Ed.* 2014, *53*, 5453−5457.

(23) Kajiwara, T.; Terabayashi, T.; Yamashita, M.; Nozaki, K. Syntheses, Structures, and Reactivities of Borylcopper and -zinc Compounds: 1,4-Silaboration of an α,β-Unsaturated Ketone to Form a γ-Siloxyallylborane. *Angew. Chem., Int. Ed.* 2008, *47*, 6606−6610.

(24) Segawa, Y.; Yamashita, M.; Nozaki, K. Boryl Anion Attacks Transition-Metal Chlorides To Form Boryl Complexes: Syntheses, Spectroscopic, and Structural Studies on Group 11 Borylmetal Complexes. *Angew. Chem., Int. Ed.* 2007, *46*, 6710−6713.

(25) Yamashita, M.; Suzuki, Y.; Segawa, Y.; Nozaki, K. Synthesis, Structure of Borylmagnesium, and Its Reaction with Benzaldehyde to Form Benzoylborane. *J. Am. Chem. Soc.* 2007, *129*, 9570−9571.

(26) Weber, L. 1,3,2-Diazaborolyl Anions − From Laboratory Curiosities to Versatile Reagents in Synthesis. *Eur. J. Inorg. Chem.* 2017, *2017*, 3461−3488.

(27) Wang, B.; Luo, G.; Nishiura, M.; Luo, Y.; Hou, Z. Cooperative Trimerization of Carbon Monoxide by Lithium and Samarium Boryls. *J. Am. Chem. Soc.* 2017, *139*, 16967−16973.

(28) Lu, W.; Hu, H.; Li, Y.; Ganguly, R.; Kinjo, R. Isolation of 1,2,4,3-Triazaborol-3-yl-metal (Li, Mg, Al, Au, Zn, Sb, Bi) Derivatives and Reactivity toward CO and Isonitriles. *J. Am. Chem. Soc.* 2016, *138*, 6650−6661.

(29) Robinson, S.; McMaster, J.; Lewis, W.; Blake, A. J.; Liddle, S. T. Alkali-metal mediated reactivity of a diaminobromoborane: mono- and bis-borylation of naphthalene versus boryl lithium or hydroborane formation. *Chem. Commun.* 2012, *48*, 5769−5771.
(30) Protchenko, A. V.; Vasko, P.; Fuentes, M. A.; Hicks, J.; Vidovic, D.; Aldridge, S. Approaching a "Naked" Boryl Anion: Amide Metathesis as a Route to Calcium, Strontium, and Potassium Boryl Complexes. *Angew. Chem., Int. Ed.* 2021, *60*, 2064−2068.
(31) Ohsato, T.; Okuno, Y.; Ishida, S.; Iwamoto, T.; Lee, K.-H.; Lin, Z.; Yamashita, M.; Nozaki, K. A Potassium Diboryllithate: Synthesis, Bonding Properties, and the Deprotonation of Benzene. *Angew. Chem., Int. Ed.* 2016, *55*, 11426−11430.
(32) Anker, M. D.; Coles, M. P. Isoelectronic Aluminium Analogues of Carbonyl and Dioxirane Moieties. *Angew. Chem., Int. Ed.* 2019, *58*, 13452−13455.
(33) Hicks, J.; Vasko, P.; Goicoechea, J. M.; Aldridge, S. Synthesis, structure and reaction chemistry of a nucleophilic aluminyl anion. *Nature* 2018, *557*, 92−95.
(34) Hicks, J.; Vasko, P.; Goicoechea, J. M.; Aldridge, S. The Aluminyl Anion: A New Generation of Aluminium Nucleophile. *Angew. Chem., Int. Ed.* 2021, *60*, 1702−1713.
(35) Koshino, K.; Kinjo, R. Construction of σ-Aromatic AlB2 Ring via Borane Coupling with a Dicoordinate Cyclic (Alkyl)(Amino)-Aluminyl Anion. *J. Am. Chem. Soc.* 2020, *142*, 9057−9062.
(36) Yang, W.; Krantz, K. E.; Dickie, D. A.; Molino, A.; Wilson, D. J. D.; Gilliard, R. J., Jr. Crystalline BP-Doped Phenanthryne via Photolysis of The Elusive Boraphosphaketene. *Angew. Chem., Int. Ed.* 2020, *59*, 3971−3975.
(37) Yang, W.; Krantz, K. E.; Freeman, L. A.; Dickie, D. A.; Molino, A.; Frenking, G.; Pan, S.; Wilson, D. J. D.; Gilliard, R. J., Jr. Persistent Borafluorene Radicals. *Angew. Chem., Int. Ed.* 2020, *59*, 3850−3854.
(38) Yang, W.; Krantz, K. E.; Freeman, L. A.; Dickie, D. A.; Molino, A.; Kaur, A.; Wilson, D. J. D.; Gilliard, R. J., Jr. Stable Borepinium and Borafluorenium Heterocycles: A Reversible Thermochromic "Switch" Based on Boron−Oxygen Interactions. *Chem. − Eur. J.* 2019, *25*, 12512−12516.
(39) Wentz, K. E.; Molino, A.; Freeman, L. A.; Dickie, D. A.; Wilson, D. J. D.; Gilliard, R. J. Reactions of 9-Carbene-9-Borafluorene Monoanion and Selenium: Synthesis of Boryl-Substituted Selenides and Diselenides. *Inorg. Chem.* 2021, *60*, 13941−13949.
(40) Hollister, K. K.; Molino, A.; Breiner, G.; Walley, J. E.; Wentz, K. E.; Conley, A. M.; Dickie, D. A.; Wilson, D. J. D.; Gilliard, R. J. Air-Stable Thermoluminescent Carbodicarbene-Borafluorenium Ions. *J. Am. Chem. Soc.* 2022, *144*, 590−598.
(41) Wentz, K. E.; Molino, A.; Freeman, L. A.; Dickie, D. A.; Wilson, D. J. D.; Gilliard, R. J. Activation of Carbon Dioxide by 9-Carbene-9-borafluorene Monoanion: Carbon Monoxide Releasing Transformation of Trioxaborinanone to Luminescent Dioxaborinanone. *J. Am. Chem. Soc.* 2022, *144*, 16276.
(42) Su, X.; Bartholome, T. A.; Tidwell, J. R.; Pujol, A.; Yruegas, S.; Martinez, J. J.; Martin, C. D. 9-Borafluorenes: Synthesis, Properties, and Reactivity. *Chem. Rev.* 2021, *121*, 4147−4192.
(43) Longobardi, L. E.; Liu, L.; Grimme, S.; Stephan, D. W. Stable Borocyclic Radicals via Frustrated Lewis Pair Hydrogenations. *J. Am. Chem. Soc.* 2016, *138*, 2500−2503.
(44) Longobardi, L. E.; Zatsepin, P.; Korol, R.; Liu, L.; Grimme, S.; Stephan, D. W. Reactions of Boron-Derived Radicals with Nucleophiles. *J. Am. Chem. Soc.* 2017, *139*, 426−435.
(45) Lavallo, V.; Canac, Y.; Präsang, C.; Donnadieu, B.; Bertrand, G. Stable Cyclic (Alkyl)(Amino)Carbenes as Rigid or Flexible, Bulky, Electron-Rich Ligands for Transition-Metal Catalysts: A Quaternary Carbon Atom Makes the Difference. *Angew. Chem., Int. Ed.* 2005, *44*, 5705−5709.
(46) Melaimi, M.; Jazzar, R.; Soleilhavoup, M.; Bertrand, G. Cyclic (Alkyl)(amino)carbenes (CAACs): Recent Developments. *Angew. Chem., Int. Ed.* 2017, *56*, 10046−10068.
(47) Soleilhavoup, M.; Bertrand, G. Cyclic (Alkyl)(Amino)Carbenes (CAACs): Stable Carbenes on the Rise. *Acc. Chem. Res.* 2015, *48*, 256−266.
(48) Bryce, D. L.; Wasylishen, R. E.; Gee, M. Characterization of Tricoordinate Boron Chemical Shift Tensors: Definitive High-Field Solid-State NMR Evidence for Anisotropic Boron Shielding. *J. Phys. Chem. A* 2001, *105*, 3633−3640.
(49) Jameson, C. J.; Gutowsky, H. S. Calculation of Chemical Shifts I. General Formulation and the Z Dependence. *J. Chem. Phys.* 1964, *40*, 1714−1724.
(50) Hermanek, S. Boron-11 NMR spectra of boranes, main-group heteroboranes, and substituted derivatives Factors influencing chemical shifts of skeletal atoms. *Chem. Rev.* 1992, *92*, 325−362.
(51) Cordero, B.; Gómez, V.; Platero-Prats, A. E.; Revés, M.; Echeverría, J.; Cremades, E.; Barragán, F.; Alvarez, S. Covalent radii revisited. *Dalton Trans.* 2008, 2832−2838.
(52) Accorsi, G.; Listorti, A.; Yoosaf, K.; Armaroli, N. 1,10-Phenanthrolines: versatile building blocks for luminescent molecules, materials and metal complexes. *Chem. Soc. Rev.* 2009, *38*, 1690−1700.
(53) Bencini, A.; Lippolis, V. 1,10-Phenanthroline: A versatile building block for the construction of ligands for various purposes. *Coord. Chem. Rev.* 2010, *254*, 2096−2180.
(54) Rothfuss, H.; Knöfel, N. D.; Tzvetkova, P.; Michenfelder, N. C.; Baraban, S.; Unterreiner, A.-N.; Roesky, P. W.; Barner-Kowollik, C. Phenanthroline�A Versatile Ligand for Advanced Functional Polymeric Materials. *Chem. − Eur. J.* 2018, *24*, 17475−17486.
(55) Kutyrev, A. A.; Moskva, V. V. Nucleophilic reactions of quinones. *Russ. Chem. Rev.* 1991, *60*, 72−88.
(56) Surya Prakash Rao, H.; Vijjapu, S. Chemistry of 9,10-phenanthrenequinone revisited: iron(iii) chloride catalyzed reactions of 9,10-phenanthrenequinone with acyclic and cyclic ketones provide furan annulated products. *RSC Adv.* 2012, *2*, 6773−6783.
(57) Milko, P.; Roithová, J. Redox Processes in the Iron(III)/9,10-Phenanthraquinone System. *Inorg. Chem.* 2009, *48*, 11734−11742.
(58) Antkowiak, W. Z.; Sobczak, A. Solvent effect on the reactivity of 1,10-phenanthroline-5,6-dione towards diazomethane. *Tetrahedron* 2001, *57*, 2799−2805.
(59) Bockman, T. M.; Perrier, S.; Kochi, J. K. Dehydrosilylation versus α-coupling in the electron-transfer of enol silyl ethers to quinones Strong solvent effect on photogenerated ion pairs. *J. Chem. Soc., Perkin Trans. 2* 1993, 595−597.
(60) Itoh, S.; Maruta, J.; Fukuzumi, S. Addition−cyclization reaction of nitroalkane anions with o-quinone derivatives via electron transfer in the charge-transfer complexes. *J. Chem. Soc., Perkin Trans. 2* 1996, 1429−1433.
(61) Itoh, S.; Nii, K.; Mure, M.; Ohshiro, Y. Novel addition of nitroalkanes to o-quinones. *Tetrahedron Lett.* 1987, *28*, 3975−3978.
(62) Wege, D. Abnormal addition of vinylmagnesium bromide to 9,10-phenanthraquinone. *Aust. J. Chem.* 1971, *24*, 1531−1535.
(63) Sauers, R. R. Single Electron Transfer and SN2 Reactions: The Importance of Ionization Potential of Nucleophiles. *J. Chem. Theory Comput.* 2010, *6*, 602−606.
(64) Neese, F. Software update: the ORCA program system, version 4.0. *WIREs Comput. Mol. Sci.* 2018, *8*, No. e1327.
(65) Frisch, M. J.; Trucks, G. W.; Schlegel, H. B.; Scuseria, G. E.; Robb, M. A.; Cheeseman, J. R.; Scalmani, G.; Barone, V.; Petersson, G. A.; Nakatsuji, H.; Li, X.; Caricato, M.; Marenich, A. V.; Bloino, J.; Janesko, B. G.; Gomperts, R.; Mennucci, B.; Hratchian, H. P.; Ortiz, J. V.; Izmaylov, A. F.; Sonnenberg, J. L.; Williams; Ding, F.; Lipparini, F.; Egidi, F.; Goings, J.; Peng, B.; Petrone, A.; Henderson, T.; Ranasinghe, D.; Zakrzewski, V. G.; Gao, J.; Rega, N.; Zheng, G.; Liang, W.; Hada, M.; Ehara, M.; Toyota, K.; Fukuda, R.; Hasegawa, J.; Ishida, M.; Nakajima, T.; Honda, Y.; Kitao, O.; Nakai, H.; Vreven, T.; Throssell, K.; Montgomery, Jr., J. A.; Peralta, J. E.; Ogliaro, F.; Bearpark, M. J.; Heyd, J. J.; Brothers, E. N.; Kudin, K. N.; Staroverov, V. N.; Keith, T. A.; Kobayashi, R.; Normand, J.; Raghavachari, K.; Rendell, A. P.; Burant, J. C.; Iyengar, S. S.; Tomasi, J.; Cossi, M.; Millam, J. M.; Klene, M.; Adamo, C.; Cammi, R.; Ochterski, J. W.; Martin, R. L.; Morokuma, K.; Farkas, O.; Foresman, J. B.; Fox, D. J. *Gaussian 16 Rev. A.03*; Gaussian, Inc.: Wallingford, CT, 2016.
(66) Glendening, E. D.; Badenhoop, J. K.; Reed, A. E.; Carpenter, J. E.; Bohmann, J. A.; Morales, C. M.; Landis, C. R.; Weinhold, F. *NBO*

6.0; Theoretical Chemistry Institute, University of Wisconsin: Madison: 2015.
(67) Marenich, A. V.; Cramer, C. J.; Truhlar, D. G. Universal Solvation Model Based on Solute Electron Density and on a Continuum Model of the Solvent Defined by the Bulk Dielectric Constant and Atomic Surface Tensions. *J. Phys. Chem. B* 2009, *113*, 6378–6396.